Seismic Response of the Temple of Pythian Apollo in Rhodes Island and Recommendations for Its Restoration

I. N. Psycharis[1(✉)], E. Avgenakis[1], I. M. Taflampas[1],
M. Kroustallaki[2], E. Farmakidou[3], M. Pikoula[3], M. Michailidou[3],
and A. Moropoulou[2]

[1] Laboratory for Earthquake Engineering, School of Civil Engineering,
National Technical University of Athens (NTUA), Athens, Greece
ipsych@central.ntua.gr
[2] School of Chemical Engineering,
National Technical University of Athens (NTUA), Athens, Greece
[3] Dodecanese Ephorate of Antiquities, Rhodes, Greece

Abstract. In this paper, the response of a restored part of the ancient Temple of Pythian Apollo under strong seismic motions is examined. The monument is located on the ancient Acropolis of Rhodes and, in its present condition, consists of a single free-standing column and a colonnade composed of three columns and an entablature. Only a few drums contain ancient parts found in the excavations, while the rest is newer material, placed during the Italian restoration of 1937-38. The examined structure corresponds to the monument after a probable restoration scenario, which accounts for the replacement of all complements that were installed during the Italian restoration with new parts from natural or artificial stone. The performed investigation concerns the response of the structure under six strong seismic excitations, chosen to be compatible with the tectonic environment and past seismic events, scaled to two levels of ground acceleration, corresponding to return periods of 500 years and 1000 years. The structural analyses were performed with the finite element software ABAQUS. The monument was modelled using three-dimensional deformable finite elements, while special attention was paid to the modelling of the mortar that connects structural members, as well as the interface between the drums, where rocking and sliding are allowed. The results of the analyses lead to various conclusions about the response of the structure under the considered seismic scenarios, including the danger of collapse of the monument, the residual displacements induced by the earthquakes, the stress levels that develop in the structure and across the interfaces and the expected damage to the structural members. Based on these results, conclusions are drawn regarding the adequacy or not of the strength capacity of the proposed new parts (natural and artificial stones and connecting mortar), while the possibility of damage to ancient parts during earthquakes is also examined. The main conclusion is that, if the structure remained undamaged, it could survive five out of six of the examined earthquakes, except of the stand-alone column which collapses in half of them. However, this is not the expected situation, since damage will occur to several new and ancient parts during a strong seismic event, increasing significantly the vulnerability of the structure and the risk of partial or total collapse.

1 Introduction

Contrary to typical masonry buildings, in which mortar is used to connect the individual stones, classical monuments are made of stone blocks which lie one on top of the other without any connecting material, except perhaps of clamps and dowels that are used in some cases. Due to this so called "dry construction", the stability of the structure to horizontal loads, like the seismically induced inertia loads, is based mainly on the friction that develops between the individual stone units.

In such "spinal" structures, rocking, sliding and wobbling occur during strong earthquakes. Therefore, the analysis of the seismic behaviour is a difficult problem, which has attracted the interest of several investigators, who have studied the response both analytically, through numerical models, and experimentally. Most investigations are restricted to the planar response only (e.g. [1–4], among others), since three-dimensional analyses are much more difficult; however, 3D analyses, which are necessary for the faithful representation of the dynamics of these systems, have also been presented (e.g. [5–8]). These studies have shown that the response is non-linear, complicated and sensitive to the parameters of the structure and the ground excitation; these characteristics are mainly attributed to the rocking response and are also observed in the simplest case of a rocking single rigid block [9]. They have also shown that classical monuments, despite their apparent instability to static horizontal loads, are generally earthquake-resistant [10], which is also proven from the fact that many classical monuments built in seismic prone areas have survived for almost 2500 years.

It is evident that the assessment of the vulnerability of a monument to future earthquakes is of major importance during a restoration process, since it can lead to the selection of the proper interventions for the enhancement of its seismic capacity. It should be noted, however, that this assessment is not straightforward nor one hundred per cent secure, due to the high sensitivity of the response to even small changes in the geometry and the ground motion characteristics. In this sense, there is an inherent uncertainty in the results and one must have in mind that, although the danger of partial or total collapse can be significantly reduced with the proper interventions, it cannot, in general, be fully eliminated.

In this paper, the seismic response of the ancient temple of Pythian Apollo, which is located at the ancient Acropolis of Rhodes, is examined. The monument (Fig. 1) consists of a single free-standing column and a colonnade, composed of three columns and an entablature. Only a few drums contain ancient parts found in the excavations, while the rest is newer material, placed during the Italian restoration of 1937–1938. The new material added during the Italian restoration consisted of tuff stones at the external part of the columns and a concrete column core, while the entablature was made of concrete. In its present condition, the monument presents significant damage, since the new material added during the Italian restoration has been cracked and deteriorated due to environmental reasons, and needs to be replaced.

Fig. 1. The current state of the temple of Pythian Apollo on the ancient Acropolis of Rhodes.

The investigation presented herein aims to provide answers to critical questions related with the restoration of the monument, such as its vulnerability to earthquakes and the required strength of the materials to be used for the construction of the complements. To this end, the proposed restoration of the monument is examined, in which the damaged Italian restoration parts are replaced with new natural or artificial stones, while complements are added to replace missing parts. In this restoration scenario, the concrete core of the columns is replaced with new stones with height equal to the height of each drum. In this way, the drums are free to rock and slide, as in the ancient structure, in contrast to the Italian restoration in which the columns behave monolithically, due to the continuous concrete core along their height.

The structural analyses were performed using the finite element software ABAQUS. The monument was modelled using three-dimensional deformable finite elements, while special attention was paid to the modelling of the mortar between the ancient and the new parts, as well as the interface between the drums, where rocking and sliding are allowed. The analyses were performed for suitable surrogate ground acceleration time histories, compatible with the tectonics and the seismicity of the region, which were selected from strong-motion databases to replicate as closely as possible past and anticipated earthquakes. For their selection, a hazard analysis was performed for the region. Analyses were performed for two intensity levels of the ground excitations, corresponding to return periods of 500 and 1000 years.

The scope of the analyses was to investigate the danger of partial or total collapse of the monument, and to derive the stress levels that will develop in the structural members during a strong earthquake. Based on the latter results, the expected damages in the ancient and the new stone parts are estimated and their effect on increasing the vulnerability of the structure is evaluated. In this way, conclusions are drawn on the adequacy or not of the strength of the proposed materials.

2 Numerical Model

During a seismic event, the response of an ancient monument is dominated by its "spinal" construction and is governed by the rocking, the sliding and the wobbling of the stone units, which may translate and rotate independently or in groups. The response continuously changes between different 'modes' of vibration, with different joints being opened each time. It is noted that the term 'mode' is used here to denote the patterns of the response and does not literally refer to the eigenmodes of the system, since spinal structures do not possess natural modes in the classical sense of structural dynamics.

The underlying mathematical problem is strongly non-linear and, consequently, the modelling of the dynamic behaviour of ancient monuments is quite complex and differs from the approaches followed in modern structural analysis. Indicatively it is mentioned that even in the simplest case of the planar response of a monolithic rocking block, the analysis is not trivial [9]. The dynamic response becomes much more complex when the three-dimensional response of a column with cylindrical drums is examined; in this case realistic models must account for non-linearities related to the three-dimensional motion of each drum (rocking, wobbling and sliding) and the energy dissipation at the joints [7, 8]. In such cases, powerful numerical codes are needed to perform the analysis.

One method that has been proven to be very efficient in dealing with such systems is the Distinct (or Discrete) Element Method (DEM) introduced by Cundall in the context of rock mechanics [11]. Alternatively, finite element implementations with joint elements (e.g. ABAQUS [12] among others) can also be used. The ability of these codes to predict the seismic response of ancient monuments with satisfactory accuracy has been validated from the comparison of numerical results with experimental data concerning the seismic (shaking table) response of a marble model of part of the colonnade of the Parthenon in a scale 1:3 [5, 13]. The analyses performed within the investigation presented herewith were made using the software ABAQUS.

Since deformation and failure of multi-block structures are mainly governed by the relative movements between blocks, the blocks can be assumed rigid without significant loss of precision. However, deformable blocks were considered in the present investigation, in order to determine the stresses induced in the stone blocks. Of course, this increased the runtimes tremendously, compared to the rigid block assemblies.

At the joints, "hard contacts" were assumed in the normal direction, which allow the development of compressive stresses only (no tension), while the penalty method was chosen to model friction in the tangential direction. The friction coefficient considered was $\mu = 0.7$, assuming that it is slightly smaller than the one for marble, for which $\mu = 0.75$ is considered a good average value [13, 14].

Joints were assumed between the drums of the columns and between the beams of the entablature. For the latter, the titanium clamps that connect the beams in the horizontal direction were modelled with inelastic truss elements, while the dowels that connect the beams in the vertical direction were modelled with equivalent linear shear springs. However, since dowels are expected to yield, even for medium-size earthquakes, the stiffness of the linear springs was assumed equal to 1/1000 of their initial

stiffness, which corresponds to spring force approximately equal to the dowels' yield force for the expected maximum relative displacement of the connected elements (about 8 cm).

The geometry of the structure was implemented in the numerical model with the best possible accuracy. To this end, the 3D digital representation of the monument (Fig. 2a), which was produced by the Photogrammetry Laboratory of NTUA using scanning technology, was used. However, due to lack of more exact information, the connection interfaces between ancient and new stones were modelled with plane surfaces. The resulting numerical model, which was used in the analyses, is shown in Fig. 2b.
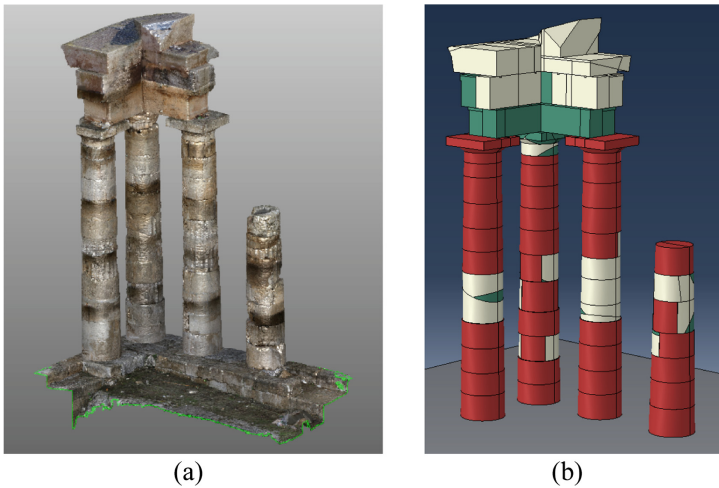

(a)   (b)

Fig. 2. (a) 3D digital reproduction of the monument; (b) Numerical model in ABAQUS. The colours denote the materials: white = ancient stone, red = new natural stone, green = artificial stone from mortar.

Table 1. Elastic mechanical properties of the materials considered in the analyses.

Property	Material	Value
Young's modulus	Ancient stone	7 GPa
	New stone	7 GPa
	Mortar	16 GPa
	Titanium clamps	105 GPa
Density	Ancient stone	2.2 Mgr/m^3
	New stone	2.0 Mgr/m^3
	Mortar	1.9 Mgr/m^3
Poisson's ratio	Ancient stone	0.25
	New stone	0.25
	Mortar	0.25

Table 2. Material strength values assumed for the checks.

Material	Property	Value
Ancient stone	Compressive strength	9.0 MPa
	Tensile strength	0.4 MPa
New stone	Compressive strength	9.0 MPa
	Tensile strength	0.4 MPa
Artificial stone mortar	Compressive strength	9.0/15.0 MPa
	Tensile strength	0.9/1.5 MPa
Connective mortar	Compressive strength	7.5/11.5 MPa
	Tensile strength	0.75/1.2 MPa
Titanium clamps	Yield stress	300 MPa
	Ultimate stress (e_u = 20%)	420 MPa

In the numerical model, different bodies were used for the ancient and the new stone, modelled using mainly hexahedral and, in few cases, second order tetrahedral elements. In cases in which pieces were connected with mortar, the layer of mortar was also modeled as an individual body of thickness 1 cm. As afore-mentioned, all bodies were assumed deformable with the properties shown in Table 1. All elements, except the horizontal titanium clamps that connect the beams of the entablature, were assumed elastic.

Since elastic behaviour was considered for the structural members, in order to predict probable failure regions, the principal stresses developing for the seismic scenarios assumed are checked against the strength of the corresponding material. The considered strength values are shown in Table 2.

For the new natural stone, the compressive strength was taken equal to 9 MPa, equal to the characteristic value obtained from compression tests on specimens from the local quarry at Sfouggaria. The corresponding characteristic tensile strength was considered equal to only 0.4 MPa, according to the results of Brazilian tests (tensile split tests) which gave a tensile strength of 0.5 MPa, which was then reduced by about 30% to obtain the strength in direct tension. However, since this value of the tensile strength was based on only six tests and is much less than the usually assumed value of 10% of the compression strength, the possibility of larger tensile strength is also considered in the evaluation of the results.

For the ancient stone, very limited information was available, specifically rebound hammer tests, which gave a mean compressive strength of 12.5 MPa with a standard deviation of 3.53 MPa. Taking under consideration that the rebound hammer tests usually overestimate the strength due to surface crystallization, and the fact that the ancient stone is of about the same quality with the new one, the strength values of the new stone were also adopted for the ancient one.

For the artificial stone made from mortar, which will be used for the construction of the beams of the entablature and of the complements of the ancient pieces, two cases were examined: (i) industrial mortar with compressive strength 15 MPa and (ii) in situ prepared mortar with compressive strength 9 MPa. For the mortar that will be used for the connections of ancient stones with new ones, two strength values were also

considered: 11.5 MPa and 7.5 MPa. For all mortars, the tensile strength was taken approximately equal to 10% of the compressive strength.

No artificial (numerical) damping was introduced to the system. According to the results of a previous investigation [13], damping can be set to zero during intense rocking response, while non-zero damping should be considered close to the tail of the ground motion in order to dissipate the free vibrations and make possible the estimation of permanent deformations. However, according to reference [14], the value of damping that is used at the end of the strong motion and the time instant that it is introduced, do not affect significantly the response and the estimation of the residual displacements. Therefore, damping was set to zero for the whole time history and only frictional dissipation of energy was considered.

3   Seismic Excitations

The base excitations that are used in numerical analyses of ancient monuments affect the results considerably. Therefore, in analyses aiming at decision making regarding interventions to monuments, suitable surrogate ground acceleration time histories should be selected, which must replicate as closely as possible past and anticipated earthquakes and be compatible with the tectonics and the seismicity of the region. To this end, for the analyses performed in the present study six earthquake records from Greece, Italy and California were selected with the following criteria:

– To have been generated by normal and reverse faults.
– To have moment magnitude between 6.5 and 7.5.
– To have been recorded on stiff ground, similar to the ground at the site.
– To have been recorded at a distance $\leq$ 20 km from the fault in order to account for the normal fault that exists a little far away from the east cost of the Rhodes island, in a distance of about 20 km from the temple of Pythian Apollo.
– To have different frequency characteristics, including near faults effects.

Concerning the last criterion, it is noted that previous studies have shown that directivity pulses inherent in ground motions recorded near the fault are extremely dangerous to ancient monuments.

The characteristics of the selected ground motions are given in Table 3. Four of the records were rotated so that the L component corresponds to the direction in which the pulse index [21] attains its maximum value.

For the dynamic analyses, the records were scaled to proper *PGA* values, compatible with the expected ground accelerations at the site of the monument. To this end, a seismic hazard analysis was performed, which was twofold: First, a probabilistic estimation of the seismic motion at the site of the monument was made using the data from the European Facility for Earthquake Hazard and Risk, EFEHR [15]; then, a deterministic approach was applied, based on the characteristics of the fault at the east cost of the island, using attenuation relationships from the United States (NGA) [17, 18] and Europe [19, 20].

Table 3. Characteristics of the considered earthquake records.

Earthquake	Date	M_w	Station	Symbol	Dist. [km]	Rotation[a]	PGA [cm/s²]	$T_{p\text{-}1}^{(b)}$ [sec]	$T_{p\text{-}1}^{(c)}$ [sec]	Scale for PGA = 0.5 g	PGA = 0.7 g
Campano Lugano, Italy	1980	6.9	Bagnoli-Irpino	BGI	8	Y	L: 183.68 T: 123.44	1.28 1.22	2.18 2.18	3.257	4.560
Northridge, California	1994	6.7	Santa Susana	SSU	17	N	L: 279.9 T: 227.1	1.08 0.58	1.90 1.94	1.945	2.724
Northridge, California	1994	6.7	L.A. 00	LA0	19	Y	L: 365.23 T: 282.52	0.74 0.54	1.50 1.16	1.527	2.138
Northridge, California	1994	6.7	L.A. Dam	LDM	6	Y	L: 462.11 T: 347.28	1.30 2.36	— 1.12	1.224	1.714
Loma Prieta, California	1989	6.9	Lexington Dam	LEX	5	Y	L: 432.85 T: 446.75	1.06 1.06	— —	1.115	1.562
Kozani, Greece	1995	6.6	Kozani	KOZ	20	N	L: 203.9 T: 139.6	1.16 0.40	0.56 1.08	2.907	4.070

(a) In rotated records, component L corresponds to the strong directivity pulse.
(b) Period of main pulse, derived from the peak of the PSV spectrum for 5% damping (for T > 0.4 s).
(c) Period of second important pulse, derived from the second peak of the PSV spectrum for 5% damping (for T > $T_{p\text{-}1}$).

Table 4. Expected peak ground acceleration (PGA) in the city of Rhodes for different return periods according to EFEHR and EC8.

Return period	Probability of exceedance in 50 years	EFEHR: PGA (g)		EC8 a_g (g)
		Average	Mean + 1 s.d.	
500 years	10%	0.51	0.62	0.24
1000 yrs	5%	0.70	0.81	0.31
2000 yrs	2.5%	0.93	1.20	0.40

In Table 4, the values of the expected peak ground acceleration (PGA) for three return periods and probabilities of exceedance according to the probabilistic analysis are given. The corresponding values according to the Greek Annex of Eurocode 8-Part 1 (EN1998-1) [16], denoted as EC8, are also provided for comparison. The deterministic analysis produced an average PGA (from all methodologies) equal to 0.59 g at a distance R_x = 20 km from the fault. Based on these results, the dynamic analyses were performed for two intensity levels of the ground excitations, corresponding to return periods of 500 and 1000 years, specifically: 0.50 g for return period 500 years and 0.70 g for return period 1000 years.

To achieve these PGA values, the original records were multiplied with the scaling factors given in the last two columns of Table 3 for PGA = 0.50 g and PGA = 0.70 g. These values were derived by equating the geometric mean of the PGA of the two horizontal components of each record with 0.50 g or 0.70 g, respectively.

The response spectra of the two horizontal components of the selected ground motions, scaled to PGA = 0.50 g, are shown in Fig. 3. In this figure, the elastic response spectra of type A of EC8 for a_g = 0.24 g and a_g = 0.36 g and for soil type A are also presented for comparison. It is noted that, according to the Greek Annex of EC8, Rhodes belongs to seismic zone Z2, for which the ground acceleration is equal to a_g = 0.24 g, while the value of a_g = 0.36 g corresponds to zone Z3. However, these

are effective ground accelerations (*EPA*s), which, in general, can be as much as 50% smaller than *PGA*s. Therefore, it can be assumed that the Code ground acceleration of $a_g = 0.24$ g corresponds to a *PGA* value around 0.36 g.
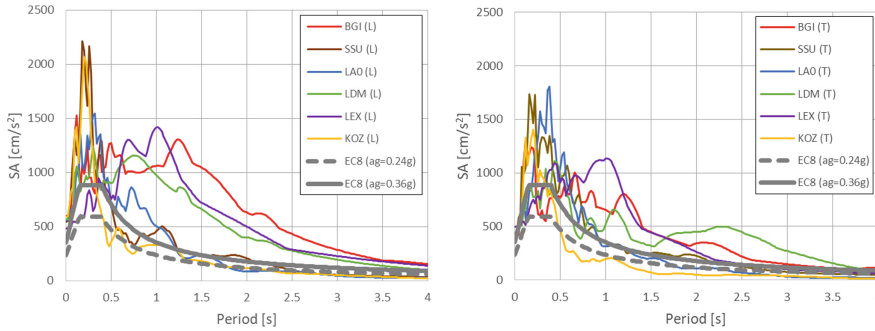

Fig. 3. Response spectra for 5% damping of the two horizontal components (L left and T right) of the selected ground motions scaled to *PGA* = 0.50 g, and comparison with the elastic spectrum of EC8 for ground type A and ground acceleration $a_g = 0.24$ g and $a_g = 0.36$ g.

The large spectral values that appear in the spectra of the records BGI, LEX and LDM for periods $T > 0.6$ s are caused by the long-period directivity pulses contained in these records (see T_{p-1} και T_{p-2} values in Table 3).

4   Results and Discussion

4.1   Damage Due to Strength Exceedance

Indicative results concerning the maximum stresses that develop in the structural members are shown in Fig. 4 for the LEX earthquake scaled to *PGA* = 0.70 g. These plots show the stress distribution in selected structural members at adverse time instances during the earthquake motion. Members denoted with 'A' refer to ancient stones, with 'N' to new stones and with 'M' to mortar, either as artificial stones or connective material. The maximum and the minimum principal stresses are presented on the left and the right column, respectively. Various colours are used to illustrate stress exceedances over the strength values shown in Table 2.

From the results depicted in Fig. 4 and from similar and additional results obtained for the other earthquake scenarios considered, the following conclusions can be drawn:

- At the columns' drums, regions, in which the tensile strength of both the ancient stone and the new stone is exceeded (brown, orange, red, yellow and grey colour, Fig. 4a, c, g, i), are observed in all earthquakes considered. In most cases, the areas with strength exceedance are restricted to a surface layer of small depth at the joint interfaces, where large normal and shear forces develop during rocking. At such places, cracks are expected to occur, which can lead to the deterioration of the
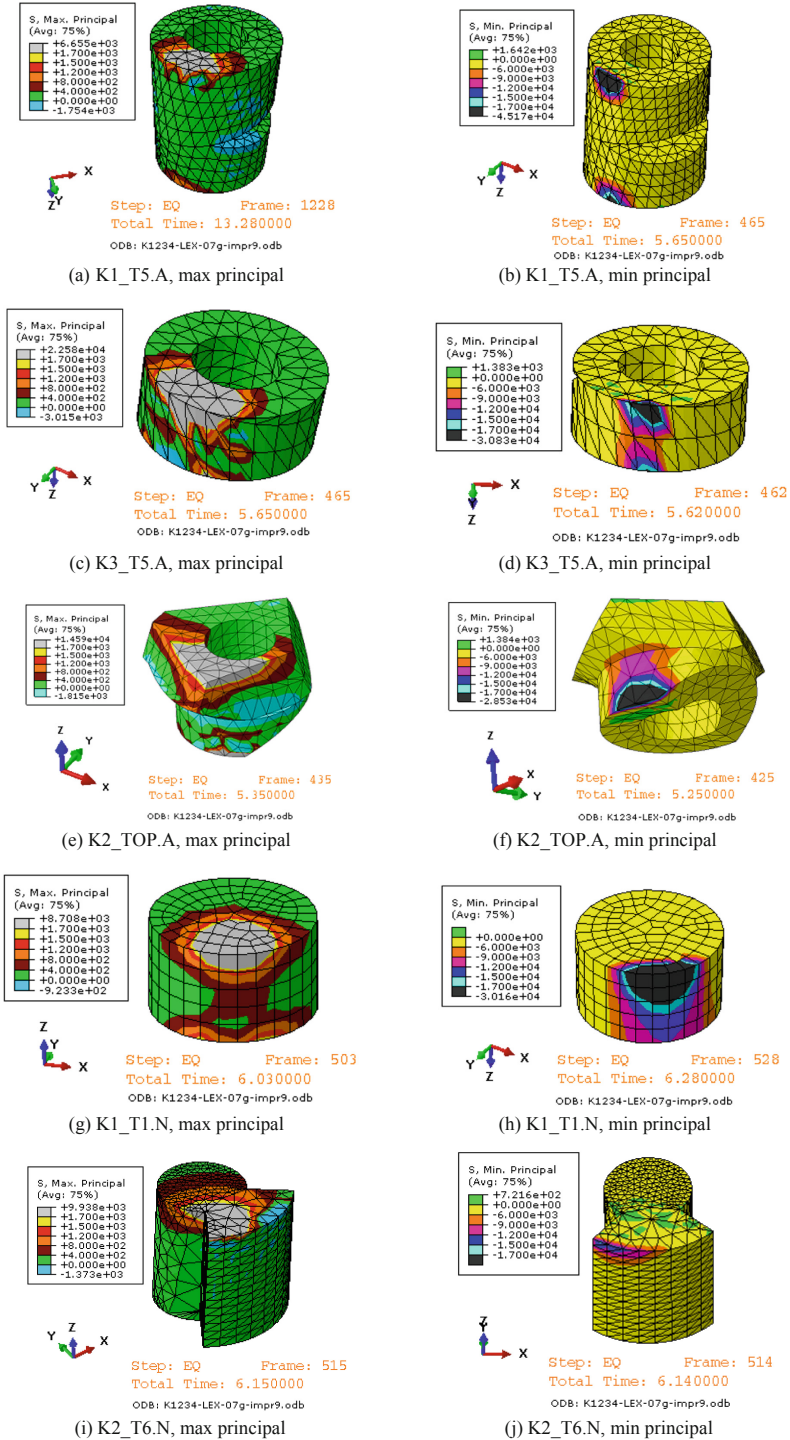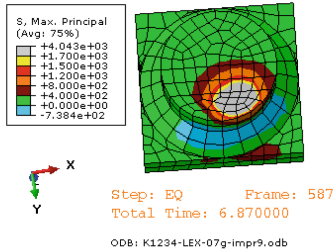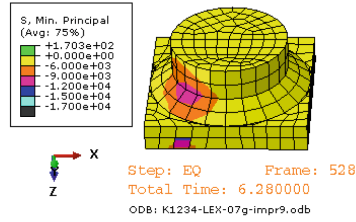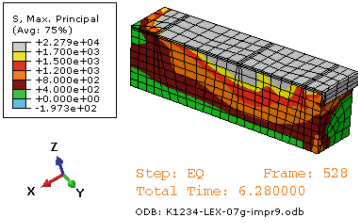
(a) K1_T5.A, max principal

(b) K1_T5.A, min principal

(c) K3_T5.A, max principal

(d) K3_T5.A, min principal

(e) K2_TOP.A, max principal

(f) K2_TOP.A, min principal

(g) K1_T1.N, max principal

(h) K1_T1.N, min principal

(i) K2_T6.N, max principal

(j) K2_T6.N, min principal

Fig. 4. Distribution of principal tensile (left) and compressive (right) stresses in selected structural elements at adverse time instances during the LEX earthquake scaled to *PGA* = 0.70 g (continues).
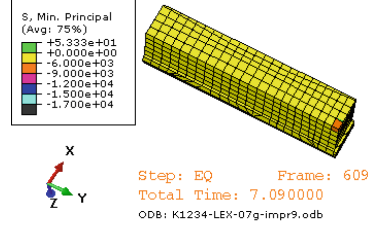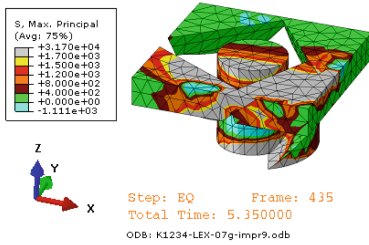
(k) K1_TOP.N, max principal
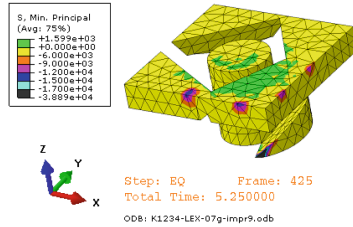

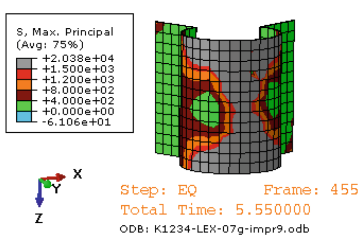(l) K1_TOP.N, min principal

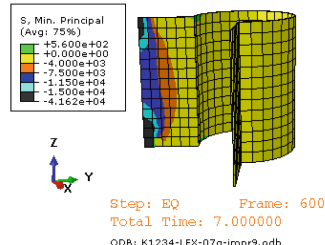(m) EPB1.M, max principal

(n) EPB1.M, min principal

(o) K2_TOP.M, max principal

(p) K2_TOP.M, min principal

(q) K2_T3.M, max principal

(r) K2_T3.M, min principal

Fig. 4. (*continued*)

contact surface, edge cut-offs and detachment of small pieces. It is noted, however, that in some cases, these areas of tensile strength exceedance are much larger, covering the whole height of the drum (Fig. 4g). In such cases, a large portion of the drum can fail and be detached, leading to loss of support for the superstructure and increased possibility of collapse. Interesting to note that, even if the tensile strength were double the value of Table 2 (i.e. 0.8 MPa instead of 0.4 MPa), the above

conclusions would not change significantly, since the areas where the tensile strength would have been exceeded would continue to be significant (orange, red, yellow and grey colour). Concerning the compressive stresses, the areas in which the compressive strength is exceeded (Fig. 4b, d, h, j, pink, blue, cyan and black colour) are generally small, implying that only limited edge cut-offs and, possibly, surface peeling (Fig. 4h) will occur.

- At the capitals of the columns, large regions showing exceedance of the tensile strength are observed in all earthquakes (brown, orange, red, yellow and grey colour, Fig. 4e, k), which imply that significant damage will occur during strong earthquakes at both the top and the bottom surfaces. Again, even if the tensile strength were double the value of Table 2, the damage to the capitals would not reduce significantly.

- The beams of the entablature will be constructed from artificial stone, either industrial mortar or in situ prepared one. In the first case (larger strength values in Table 2), quite large areas, where the tensile strength is exceeded, are observed (Fig. 4m, yellow and grey colour). In most cases, these areas are restricted to a surface layer of small depth at the joint interfaces where cracks are expected to occur, which can lead to the deterioration of the contact surface, edge cut-offs and detachment of small pieces. However, in some earthquakes larger areas with strength exceedance develop (as in case of Fig. 4m), which can lead to more severe damage and partial loss of support for the beams above. Evidently, if in situ prepared mortar of smaller strength (smaller strength values in Table 2) will be used, the damage will increase (areas with orange, red, yellow and grey colour in Fig. 4m). These results show that reinforcement rebars are needed to enhance the tensile capacity of the beams.

- Similar conclusions can be drawn for the complements that will be constructed with artificial stone (e.g. the complements of the ancient capital of the corner column): Large principal tensile stresses develop, larger than the tensile strength, which can lead even to their failure (Fig. 4o, yellow and grey colour for industrial mortar, orange, red, yellow and grey colour for in situ prepared mortar).

- Significant damage is also expected to occur during a strong earthquake to the mortar that will be used to connect ancient with new stones. As shown in Fig. 4q, large areas, in which the tensile strength is exceeded, develop (red and grey colour for tensile strength 1.2 MPa, orange, red and grey colour for tensile strength 0.8 MPa), which will lead to extensive cracking of the mortar and detachment of the connected members. Note that the stresses shown in Fig. 4q have been derived assuming that the bond between the mortar and the stone is strong enough and will not fail. However, tests performed to check the bond between the mortar and the new stone showed very small bond capacity; therefore, the bonds are expected to fail before the mortar. In any case, these results show that reinforcement with titanium bars is required to guarantee the integrity of the connected members.

- Finally, in what concerns the horizontal clamps that connect the beams of the entablature, the results show that they yield in some of the ground motions

examined; however they do not break. Larger forces develop at the clamps of the corner, where permanent dislocations of the beams are expected to occur due the plastic deformation and the residual displacements of the clamps.

4.2   Overall Stability

Regarding the overall stability of the monument, there are seismic scenarios in which part or the whole monument collapses, even if one ignores the damage induced by the aforementioned stress exceedances. The free-standing column collapsed in three out of the six ground motions examined, even for $PGA = 0.5$ g, while the three connected columns collapse only under the BGI earthquake for both PGA values. Indicative snapshots showing the deformed shape of the monument during the seismic excitations considered, scaled to $PGA = 0.50$ g are presented in Fig. 5.

It is noted that, as mentioned above, significant damage is expected to occur to the drums of the columns during a severe seismic event. Therefore, the actual overall stability of the monument is smaller than the one depicted in Fig. 5, since partial or
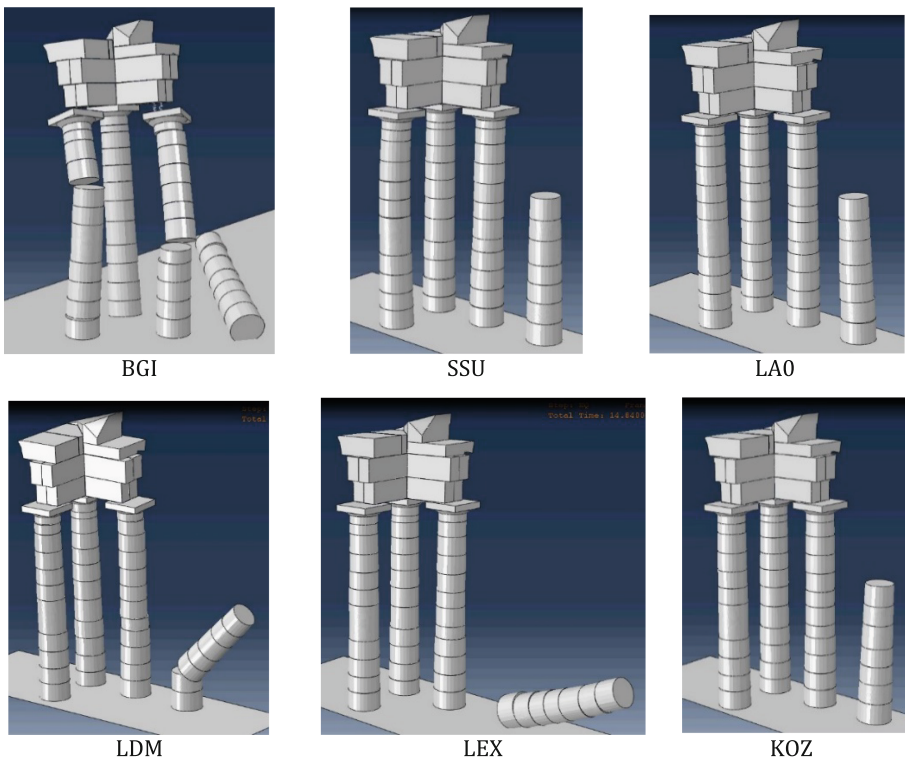

Fig. 5. Snapshots of the response for the ground motions scaled to $PGA = 0.5$ g. The free-standing column collapses in earthquakes BGI, LDM and LEX, while the three connected columns collapse only in BGI.

total collapse might also be triggered by the partial failure of the drums or the detachment of connected parts, which will lead to loss of support of the superstructure.

The fact that the ground motions BGI, LDM and LEX are more dangerous than the other earthquakes considered is attributed to the long-period pulses contained in these records, as evident from the large spectral values for periods around 1 s (Fig. 3). Such pulses, inherent in near-fault ground motions, are quite dangerous for the stability of ancient monuments. Also, the fact that the free-standing column is more vulnerable than the three columns connected with the entablature was expected, not only because the connection of the columns with the architraves makes them more stable, but also, because the stand-alone column has smaller size than the other columns.

4.3   Comparison with Existing Damage

It should be noted that the stress exceedances predicted by the numerical model match the existing damage in the ancient parts of the monument, confirming that the results are realistic and the predicted damage can indeed occur during a strong seismic event. Some characteristic cases are presented in Fig. 6, which are discussed in the following.

– In Fig. 6a, the area coloured with pink, blue, cyan and black denotes exceedance of the compressive strength of the stone, implying that the corresponding pieces will be cut off. Such cut-offs of edges are observed in several ancient drums (Fig. 6b) showing that such strength exceedances should have happened during past earthquakes.
– Figure 6c shows a case in which the compressive strength of the stone is exceeded in a wedge-shaped area at the side surface of the drum (pink, blue, cyan and black colour), implying that significant cracking will occur to this area, which can lead to the peeling off of the material. Such wedge-shaped peeled off areas on the side surface of ancient drums are observed in the monument (Fig. 6d) and are attributed to similar large compressive stresses developed during past earthquakes.
– Figure 6e shows a case in which principal tensile stresses, larger than the tensile strength, develop in a large portion of a drum, indicating that a significant portion of it will be severely cracked. If this happens, only part of the initial drum will remain on the structure. Probably, this is the reason that many portions of drums were found in the ruins of the monument, which were complemented with new stone during the Italian restoration (Fig. 6f: the ancient part is the one with the flutes). It is noted that this is not common in case of marble temples, where, usually, the drums of the columns are found in whole.
– The numerical results show that extended damage occurs to the capitals, due to excessive tensile stresses that develop. As shown in Fig. 6g (areas with brown, orange, yellow and grey colour), the damage will be in the form of deterioration of the upper surface and edge cut-off at the base. Interestingly enough, this type of damage matches exactly the existing damage in the ancient capital of the corner column (Fig. 6h), implying that, most probably, it occurred due to similar large stresses developed during past earthquakes.
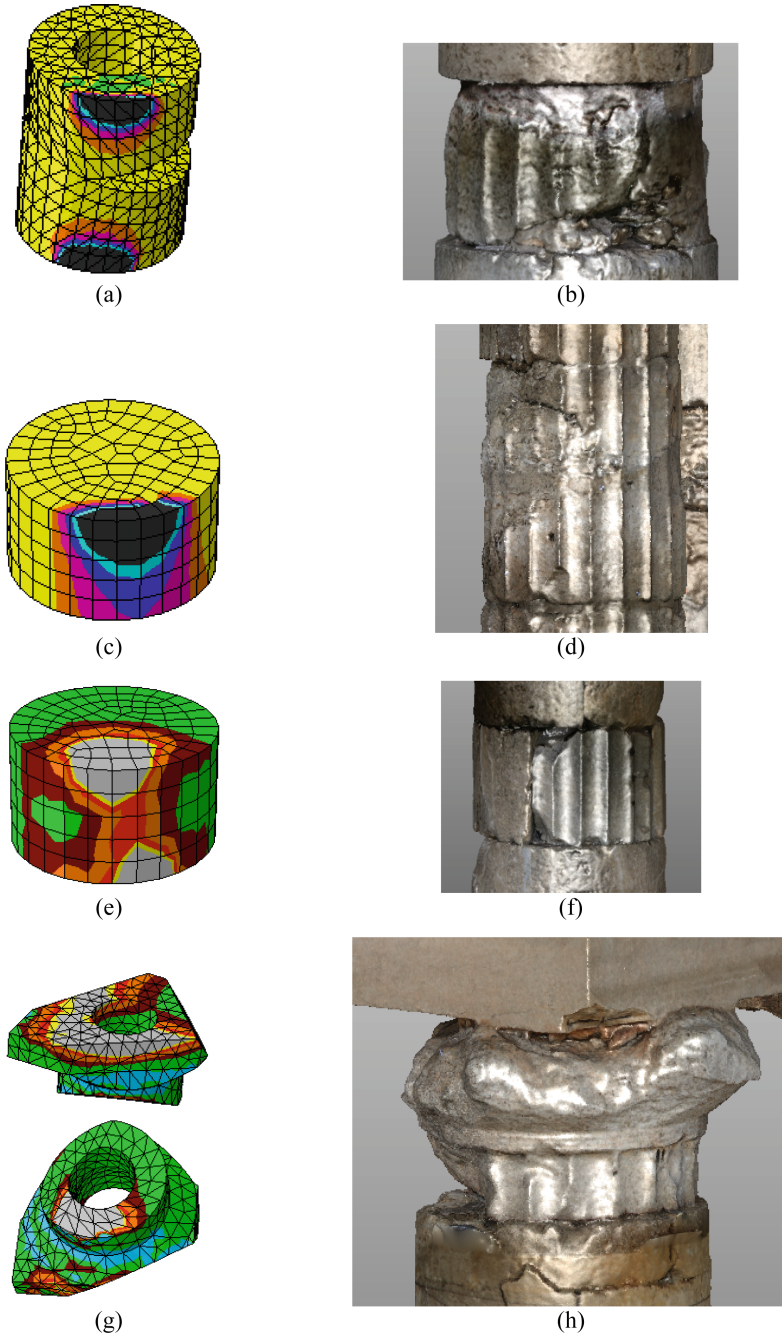
(a)   (b)

(c)   (d)

(e)   (f)

(g)   (h)

Fig. 6. Left column: areas of exceedance of the tensile or the compressive strength, according to the numerical results. Right column: existing damage in ancient members attributed to such strength exceedance during past earthquakes.

5   Conclusions

In this paper, the structural response of the ancient Temple of Pythian Apollo under six earthquake scenarios is examined. The examined structure corresponds to the restored monument, after replacement of the damaged Italian restoration parts with new natural or artificial stone and the addition of the necessary complements. The considered ground motions are compatible with the tectonics and the seismic history of the region and cover a wide range of frequency characteristics. For the analyses, the ground motions were scaled to two intensity levels: *PGA* = 0.50 g corresponding to earthquakes with average return period 500 years and *PGA* = 0.70 g corresponding to earthquakes with return period 1000 years. The main conclusions drawn are:

- In all earthquake scenarios examined, exceedances regarding both the tensile and the compressive stresses, with respect to the strength values assumed for the ancient and the new materials, are observed. Such stress exceedances occur in almost all members, including column drums and capitals, connective mortar, as well as the beams of the entablature, and are expected to result not only in local cracking and small edge cut-offs, but, in some cases, also in through-and-through cuts, which can lead to partial or total collapses.
- The expected damage is verified from the existing damage in the ancient parts.
- Due to the low strength and adhesion of the connective mortar with the ancient and new materials, addition of reinforcement is deemed necessary in the respective interfaces to ensure the integrity of the connected pieces during the seismic excitation.
- Even if one neglects the damage to stone blocks, produced by the aforementioned stress exceedances, the survival of the monument to all ground motions examined cannot be guaranteed. Specifically, the free-standing column collapses in three out of the six earthquakes considered, even for PGA = 0.5 g, which shows the high vulnerability of this column, while the three connected columns withstand five out of the six earthquakes, although with significant residual displacements. Evidently, the actual danger of collapse is larger due to the afore-mentioned expected damages to the structural members, mainly to the drums of the columns.
- The monument is more vulnerable to seismic excitations containing long-period pulses, which originate from near-fault earthquakes. Such earthquakes can be generated at the fault located 20 km east from the monument.

These conclusions show that both the ancient and the new natural stone, but also the artificial mortar stone, are of poor quality and do not have the required strength to withstand the large stresses that develop during strong earthquakes. Therefore, in a severe seismic event, significant damage to both ancient and new members are expected to occur, while the possibility of a partial or total collapse of the monument cannot be eliminated, even if the mechanical properties of the materials will be enhanced, e.g. by grouting.

Of course, these conclusions have to be re-evaluated in case that it will be decided to reconstruct the whole monument with new stone of better quality. Even in that case, however, the possibility of collapse during an earthquake cannot be excluded.

References

1. Allen, R.H., Oppenheim, I.J., Parker, A.R., Bielak, J.: On the dynamic response of rigid body assemblies. Earthq. Eng. Struct. Dyn. **14**, 861–876 (1986)
2. Konstantinidis, D., Makris, N.: Seismic response analysis of multidrum classical columns. Earthq. Eng. Struct. Dyn. **34**, 1243–1270 (2005)
3. Psycharis, I.N.: Dynamic behaviour of rocking two-block assemblies. Earthq. Eng. Struct. Dyn. **19**, 555–575 (1990)
4. Sinopoli, A.: Dynamic analysis of a stone column excited by a sine wave ground motion. Appl. Mech. Rev. **44**, S246 (1991)
5. Dasiou, M., Psycharis, I.N., Vayas, I.: Verification of numerical models used for the analysis of ancient temples. In: Prohitech Conference, Rome (2009)
6. Psycharis, I.N., Lemos, J.V., Papastamatiou, D.Y., et al.: Numerical study of the seismic behaviour of a part of the Parthenon Pronaos. Earthq. Eng. Struct. Dyn. **32**, 2063–2084 (2003)
7. Stefanou, I., Psycharis, I.N., Georgopoulos, I.: Dynamic response of reinforced masonry columns in classical monuments. Constr. Build. Mater. **25**, 4325–4337 (2011)
8. Stefanou, I., Vardoulakis, I., Mavraganis, A.: Dynamic motion of a conical frustum over a rough horizontal plane. Int. J. Non Linear Mech. **46**, 114–124 (2011)
9. Housner, G.W.: The behavior of inverted pendulum structures during earthquakes. Bull. Seismol. Soc. Am. **53**, 403–417 (1963)
10. Psycharis, I.N., Papastamatiou, D.Y., Alexandris, A.P.: Parametric investigation of the stability of classical columns under harmonic and earthquake excitations. Earthq. Eng. Struct. Dyn. **29**, 1093–1109 (2000)
11. Cundall, P.A.: Formulation of a three-dimensional distinct element model - part I: a scheme to detect and represent contacts in a system composed of many polyhedral blocks. Int. J. Rock Mech. Min. Sci. **25**, 107–116 (1988)
12. ABAQUS: User's Manual. Hibbitt, Karlsson and Sorensen Inc. (2009)
13. Papantonopoulos, C., Psycharis, I.N., Papastamatiou, D.Y., et al.: Numerical prediction of the earthquake response of classical columns using the distinct element method. Earthq. Eng. Struct. Dyn. **31**, 1699–1717 (2002). https://doi.org/10.1002/eqe.185
14. Toumbakari, E., Psycharis, I.N.: Parametric investigation of the seismic response of a column of the Aphrodite Temple in Amathus, Cyprus. In: 14th European Conference on Earthquake Engineering (2010)
15. EFEHR: European Facility for Earthquake Hazard and Risk. http://www.efehr.org
16. European Committee for Standardization (CEN): Design of structures for earthquake resistance – part 1: general rules, seismic actions and rules for buildings. EN 1998-1. Greek Annex (2004)
17. Stewart, J.P., Archuleta, R.J., Power, M.S.: Earthquake spectra issue about NGA (guest editors). Earthq. Spectra **24**, 341 (2008)

18. Bozorgnia, Y., Abrahamson, N.A., Al Atik, L., Ancheta, T.D., Atkinson, G.M., Baker, J.W., Baltay, A., Boore, D.M., Campbell, K.W., Chiou, B.S.-J., Darragh, R., Day, S., Donahue, J., Graves, R.W., Gregor, N., Hanks, T., Idriss, I.M., Kamai, R., Kishida, T., Kottke, A., Mahin, S.A., Rezaeian, S., Rowshandel, B., Seyhan, E., Shahi, S., Shantz, T., Silva, W., Spudich, P., Stewart, J.P., Watson-Lamprey, J., Wooddell, K., Youngs, R.: NGA-West2 research project. Earthq. Spectra **30**(3), 973–987 (2014)
19. Bindi, D., Pacor, F., Luzi, L., Puglia, R., Massa, M., Ameri, G., Paolucci, R.: Ground motion prediction equations derived from the Italian strong motion database. Bull. Earthq. Eng. **9**(6), 1899–1920 (2011)
20. Akkar, S., Sandikkaya, M.A., Bommer, J.J.: Empirical ground-motion models for point- and extended-source crustal earthquake scenarios in Europe and the Middle East. Bull. Earthq. Eng. **12**(1), 359–387 (2014)
21. Kardoutsou, V., Taflampas, I., Psycharis, I.N.: A new pulse indicator for the classification of ground motions. Bull. Seismol. Soc. Am. **107**(3), 1356–1364 (2017)